RSC Advances

ROYAL SOCIETY OF CHEMISTRY

www.rsc.org/advances

Cite this: DOI: 10.1039/c0xx00000x

www.rsc.org/xxxxxx

PAPER

Supercritical CO_2 Extraction of Organic Carbonate-based Electrolytes of Lithium-ion Batteries

Yuanlong Liu, Deying Mu, Rujuan Zheng and Changsong Dai*

Received (in XXX, XXX) XthXXXXXXXXX 20XX, Accepted Xth XXXXXXXXX 20XX

DOI: 10.1039/b000000x

Supercritical fluid extraction (SFE) was applied to reclaim organic carbonate-based electrolytes of spent Lithium-ion batteries. To optimize the SFE operational conditions, the response surface methodology was adopted. The parameters studied were as follow: pressure, ranging from 15 to 35MPa; temperature, between 40℃ and 50℃ and static extraction time, within 45 to 75min.The optimal conditions for extraction yield were 23MPa, 40℃ and dynamic extracted 45min. Extracts were collected at a constant flow rate of 4.0L/min. Under these conditions, the extraction yield was 85.07±0.36%, which well matched with the predicted value. Furthermore, the components of the extracts were systematically characterized and analyzed by using FT-IR, GC-MS and ICP-OES, and the effect of SFE on the electrolyte reclamation was evaluated. The results suggest that the SFE is an effective method for recovery organic carbonate-based electrolytes from spent lithium-ion batteries to prevent environmental pollution and resource waste.

Introduction

Lithium-ion batteries (LIBs) are widely used as electrochemical power sources in consumer electronics, electric vehicles and other modern-life appliances. LIBs will probably be sent to recycling facilities at the end of life which specialized in the specific battery type. As is known, spent LIBs contain lots of valuable chemical substances, besides cathode active material, also comprise copper and aluminium foil (anode and cathode current collect) and electrolyte. The electrolyte is the most valuable component except cathode material in LIBs.[1] Many recycling methods for the spent LIBs have been reported. [2-5] Mostly their concern was valuable metals while the remainder of the battery including the electrolyte was deemed worthless and disposed in any way possible to rid them.

In addition to the profit motive, there is the need for preventing the pollution caused by the hydrolysis of conductive salt and also the toxic electrolyte mixture that virtually corrupts the earth and water for any use whatever along with the danger to animal and insect life as well as human life. The electrolytes in present LIBs are mixtures which contain aprotic solvents in addition to a conductive salt. The most frequently used solvents are propylene carbonate, ethylene carbonate, diethyl carbonate and dimethyl carbonate. [6-8] Although a whole series of conductive salts is being discussed, $LiPF_6$ is by far the mostly used one.[9] On being exposed to water or moist air, $LiPF_6$ can readily hydrolyze and produce toxic hydrogen fluoride gasses. When connected with moisture, including skin tissue, hydrogen fluoride gasses immediately convert to hydrofluoric acid, which is highly corrosive to battery reclaiming facilities and toxic to operator. Obviously, it is necessary to separate or remove of spent LIBs electrolytes in a manner before the dismantling LIBs by reclaiming facilities. That can prevent above mentioned pollution and hazards.

Several electrolyte separation and extraction techniques have been employed in recycling process of spent LIBs. Lian immersed mechanical shredded LIBs into a suitable solvent for several hours, the electrolytes were extracted. The solvents were recovered by evaporation at the process of pressure reducing, and the pure electrolytes left eventually. [10] The limitations are that the solvent boiling point at reduced pressure must below the lithium salt decomposition temperature (≤80℃), and the materials are available in an anhydrous state. Similarly, Schmidt et al. developed a suitable solvents like 1, 2-dimethoxyethane, dimethyl carbonate, ethyl acetate and acetone to extract the organic electrolyte solvents, polyvinylidene fluoride and other binders, and the dissolved lithium hexafluorophosphate. The solvents used for the extraction can be recovered by reduced pressure distillation. [11] For Sun et al., electrolytes of spent LIBs were separated from LIBs using vacuum pyrolysis process in a pyrolysis system at following conditions: temperature of 600℃, vacuum evaporation time of 30min, and residual gas pressure of 1.0 kPa. The components of pyrolysis products were analyzed by FT-IR, which indicated that the main components are fluorocarbon organic compounds. [12] Most of the fluorinated compound can be enriched and recovered so as to prevent environmental pollution and resource waste. Organic solvent extraction process is always introduced a solvent impurity, which not only complicated separation process but also brought new pollutants. In vacuum pyrolysis process, electrolytes

are thoroughly decomposed in vacuum pyrolysis process, and the components of decomposition products are too complicated to reuse.

SFE is a separation technology using the relationship of density to dissolving capacity of supercritical fluid. SFE offers extraction yield comparable with those obtained by conventional extraction methods of organic solvents. In supercritical fluid systems, CO_2 has a moderate critical pressure (73.8 atm) and a low critical temperature (31.1℃) as compared to the others. [13] Under supercritical state, CO_2 has a large dissolving capacity of low and non-polar substances. [14] The CO2 are easily separated from the extract for its high volatility and can be fully recyclable and reusable without hazardous solvent wastes emission. A number of experiments have been carried out to eliminate toxic materials from waste by supercritical CO_2 extraction.[15,16] Therefore, supercritical CO_2 extraction has become a more viable option in separation industry and environmental protection industry. Leaching of spent LIBs by supercritical CO_2 and several other supercritical fluids for removal of the electrolytes were illustrated in a patent by Sloop. [17] The batteries were placed in an extraction vessel, which full of fluids. Both of the temperature and the pressure of the fluids in the extraction vessel were adjusted to achieve the supercritical state. The electrolytes were exposed to and extracted by the fluids at supercritical state. All supercritical fluids were then transferred to collection vessel where the temperature and the pressure of the fluids reverted to original state, and electrolytes left eventually. There is little information available in the patent about optimization of extraction process and component analysis of extraction product.

In this paper, the organic carbonate-based electrolytes were separated by using supercritical CO_2 from LIBs separator, simulating electrolyte extraction from the spent Lithium-ion battery. The extraction parameters were optimized with the response surface methodology (RSM) in order to obtain a considerable extraction yield in an economical operation range. Furthermore, the effect of SFE on the electrolyte reclamation was evaluated from the aspect of consistency and integrity of electrolyte components.

Experimental

Reagent and materials

The TC-E201# electrolyte mainly composed of 1 M $LiPF_6$ in EC/DMC/EMC (1:1:1 vol%) was kindly provided by Tinci Materials Technology Co., Ltd. (Guangzhou, China). Commercial grade CO_2 supplied by Liming Gas Co., Ltd. (Harbin, China), was used with the purity of more than 99.95%. The JH ordinary type polypropylene separator was purchased from Jinhui Hi-tech Optoelectronic Material Co., Ltd. (Foshan, China), which used as adsorbent of electrolytes.

Extraction procedures

For each extraction experiment, electrolytes were adsorbed in Lithium-ion battery separator, and enclosed into the extraction vessel in an argon-filled glove box with moisture and oxygen level less than 1 ppm. The extraction vessel was transferred to *Spe-ed* SCF Prime supercritical CO_2 extraction system (Applied Separations, Inc., Allentown, PA, USA) for electrolyte extraction. A schematic diagram of the apparatus is shown in Figure 1. To study the influence of pressure, temperature and time on extraction efficiency, a series of experiments was designed to conduct under the pressure from 15 to 35 MPa, the temperature from 40 to 50℃ and static extracted time from 45 to 75 min. In all experiments, the designed temperature was lower or equal to 70 ℃, the temperature employed in $LiPF_6$, since thermal degradation could take place at higher temperatures.[18] The extracts were then collected into a sample vial at a constant flow rate of 4.0 L/min. The collected sample was tightly sealed and stored in the glove box before analysis. The extraction yield was calculated according to the following equation:

$$Y\% = (m_{ads}-m_{res})/(m_{ads}-m_{sep}) \times 100 \quad (1)$$

Where Y is the extraction yield, m_{sep} is the mass of separator, m_{ads} the mass of separator after adsorbing electrolytes and m_{res} the mass of residues after extraction.

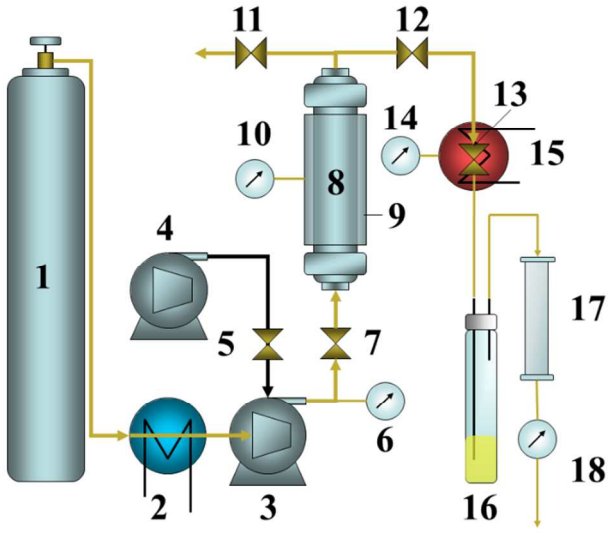

Fig. 1 Schematic diagram of supercritical CO_2 extraction apparatus: 1 CO_2 Cylinder, 2 Cooling Bath, 3 Air Driven Fluid Pump (gas booster pump), 4Air Compressor, 5 Air Regulator, 6 CO_2 Pressure, 7 Inlet Valve, 8 Extraction Vessel, 9 Heating Jacket, 10 Vessel Heat, 11 Vent Valve, 12 Outlet Valve, 13 Flow Valve, 14 Valve Heat, 15 Heating Jacket, 16 Collecting Vial, 17 Alumina filter, 18 Gas Flow meter

Experimental design

In this research, response surface methodology with Box-Behnken[19,20] design was applied to optimization of extraction conditions, which obtain the maximum extraction yield from Lithium-ion battery separator in SC-CO_2 medium. The variables studied were pressure (MPa, X_1), temperature (℃, X_2) and extraction time (min, X_3), and each variable set three levels. A total of 15 experiments were designed in Table 1, including the triplicate runs for the center point (Runs 3, 6 and 14). The center points provide an internal estimate of pure error used to test for lack of fit and also contribute toward estimation of the squared terms. All the experiments were done in triplicate and the average extraction yield (%) was taken as the response Y. The experimental data obtained were fitted to a second order polynomial equation. The equation, coefficient of determination, analysis of variance (ANOVA), surface plot and conditions for maximum extraction yield were obtained by using Design-Expert

8 (Stat-Ease, Inc., Minneapolis, MN, USA).

Table 1 Box-Behnken design and observed responses[a]

Run	Independent variable			Response (*Y*%)
	X_1 (Press, MPa)	X_2 (Temperature,)	X_3 (Time, min)	
1	15(−1)	50(+1)	60(0)	83.98
2	25(0)	40(−1)	75(+1)	86.71
3	25(0)	45(0)	60(0)	87.96
4	15(−1)	45(0)	75(+1)	84.17
5	25(0)	40(−1)	45(−1)	85.69
6	25(0)	45(0)	60(0)	87.53
7	25(0)	50(+1)	75(+1)	88.98
8	15(−1)	40(−1)	60(0)	82.24
9	35(+1)	40(−1)	60(0)	86.84
10	35(+1)	50(+1)	60(0)	88.26
11	35(+1)	45(0)	45(−1)	86.13
12	35(+1)	45(0)	75(+1)	87.72
13	15(−1)	45(0)	45(−1)	81.66
14	25(0)	45(0)	60(0)	87.55
15	25(0)	50(+1)	45(−1)	86.74

[a]Average of triplicate experiments.

Analytical methodology

IR spectra were collected on a Perkin Elmer Spectrum One FT-IR spectrometer (Waltham, MA, USA) equipped with a KBr crystal in the absorbance mode range from 400 to 4000 cm^{-1} with a resolution of 4 cm^{-1}.

The extracts were analyzed using an Agilent (Agilent Technologies, Palo Alto, CA, USA) GC-MS system (GC 6890N, MS 5973N) with a DB-5ms capillary column (30 m × 0.25 mm i.d., 1.0 μm film thickness; J&W Scientific, Folsom, CA, USA). The GC operating conditions were as follows: column temperature 60℃ maintained for 3 min, then increased to 300 ℃ at a rate of 10 ℃/min and finally sustained at 300℃ for 2 min; carrier gas helium at a flow rate 1.0 mL/min; injector temperature 280℃; injected volume 2 μL; splitless. The temperature of the transfer line was 260℃. The MS operating conditions were: ionization voltage 70 eV; ion source temperature 230℃; mass range 15-750 amu.

The concentration of $LiPF_6$ in the electrolyte solution and extract was obtained by measuring the Li^+ concentration in back-extraction solution. The $LiPF_6$ in organic liquid was extracted back to the water which the pH < 1, and the concentration of lithium ions in water was accurately analyzed by inductively coupled plasma optical emission spectrometry (ICP-OES, PerkinElmer Optima 5300DV, PerkinElmer, Waltham, Ma, USA).

^{19}F NMR (376.4 MHz, Acetone-d6, 25℃) and ^{31}P NMR (161.9MHz, Acetone-d6, 25℃) spectra were recorded on an Avance Ⅲ 400 MHz digital NMR spectrometer using either 5 mm glass tubes (Wilmad Glass Co., Buena, NJ,USA).

Results and discussion

Optimization of the experimental conditions

The supercritical CO_2 extraction of organic carbonate-based electrolytes from Lithium-ion battery separators were optimized by varying operating parameters according to the Box-Behnken design. The number of experiments needed to investigate the above mentioned three parameters at three levels would be 27 (3^3factorial). Thus, this was reduced to 15 using a Box-Behnken experimental design. The results of this limited number of experiments provided a statistical model that was used to identify trends in high yield for the extraction process. Table 1 presents the experiment design and corresponding response yield data for SFE. The analysis of variance (ANOVA) for the experimental results of the Box-Behnken design is shown in Table 2. The fit of the model can be checked by the determination coefficient (R^2), which was 0.9944, indicating that the model adequately represented the real relationship between the chosen parameters. The lack-of-fit measures the failure of the model to represent data in the experimental domain at points which are not included in the regression. The non-significant value of lack-of-fit ($p>0.05$) revealed that the model equation was adequate for predicting the yield under any combination of values of the variables. Eq. (2) illustrates the relationship of the three variables and *Y*.

$$Y=+87.61+2.11X_1+0.81X_2+0.92X_3-0.23X_1X_3+0.31X_2X_3-2.22X_1^2-0.52X_3^2 \quad (2)$$

Where Y is the extraction yield, X_1 is the pressure, X_2 the temperature and X_3 the time of extraction.

Table 2 Analysis of variance (ANOVA) for the experimental results

Source	Sum of Squares	df	Mean Squares	*F* Value	*p*-value Prob>*F*
Model	67.11	7	9.59	176.42	<0.0001
X_1	35.70	1	35.70	656.93	<0.0001
X_2	5.25	1	5.25	96.58	<0.0001
X_3	6.77	1	6.77	124.60	<0.0001
X_1X_3	0.21	1	0.21	3.89	0.0891
X_2X_3	0.37	1	0.37	6.85	0.0346
X_1^2	18.32	1	18.32	337.07	<0.0001
X_3^2	1.01	1	1.01	18.54	0.0035
Residual	0.38	7	0.054		
Lack of fit	0.26	5	0.053	0.89	0.6040
Pure Error	0.12	2	0.059		
Cor Total	67.49	14			
Adjust-R^2	0.9887				
R^2	0.9944				

Eq. (2) shows that extraction yield depends more on pressure variations followed by extraction time variation. Dependence of yield on temperature is least. In order to get a better understanding of the influences of the independent variables and their interactions on the dependent variables, three-dimensional (3D) response surface plots for the measured responses were constructed according to Eq.(2). Since the regression model has three independent variables, one variable was held constantly at the central level for each plot. Figure 2 shows the 3D response surfaces as the functions of two variables at the centre level of other variables, respectively.

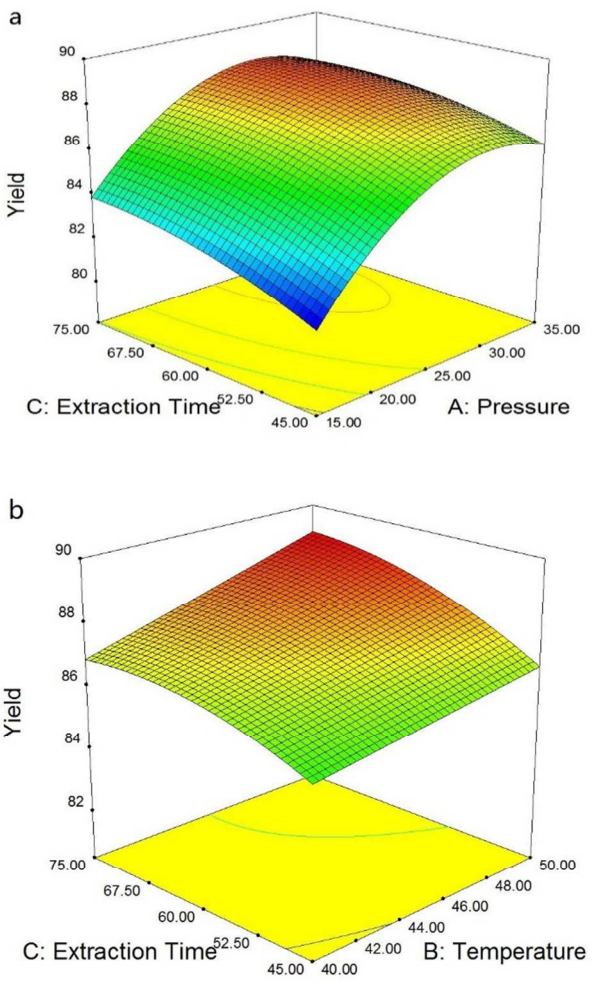

Fig. 2 Response surfaces and contour plots for: (a) Extraction time vs. Pressure; (b) Extraction time vs. Temperature.

It is generally believed that the solubility of a solute in the SCF tends to increase with the density of the fluid (at constant temperature). In present study, the influence of pressure on the composition of electrolytes displayed that, in a definite extraction time, the extraction yield was increased drastically with the pressure increasing. This result was predictable since raising the extraction pressure resulted in a higher fluid density, which can improve the solubility of the electrolyte composition. The variation of temperature during the SFE affects the fluid density and the volatility of the electrolytes from the Lithium-ion battery separator. By increasing the temperature, the volatilities of the electrolyte composition keeps an upward tendency but the SCF density decreases. In the temperature range of this study, raising temperature steadily increases the extraction yield of electrolytes due to the enhanced volatilities of the electrolyte composition.

In practice, getting the required output with minimum input is the most economical production mode. Based on the polynomial regression model, the mildest experimental conditions of considerable extraction yield were found to be at 23.4MPa, 40℃ and 45min. Under these conditions, the predicted extraction yield was 85.22%.On the basis of these results, a set of verification experiments (3 replicates) were carried out at 23 MPa, 40℃and 45min, when the average extraction yield was 85.07±0.36%. This result indicated that the experimental values were in good agreement with the predicted values, and also suggested that the model was satisfactory and accurate.

Composition analysis

Organic solvent

The appearance of extracts collected by the sample vialis a colourless liquid with a mild odour. The FT-IR spectrum (Fig. 3) of the extracts shows peaks around 3421 cm^{-1} attributed to ν_{O-H} of intermolecular hydrogen bonds, broad ν_{C-H} peaks in the range 3163-2963 cm^{-1}, typical peaks around 1805-1776 cm^{-1} attributed to $\nu_{C=O}$ of organic carbonate, typical peaks around 1597 and 1553 cm^{-1} attributed to skeletal C=C vibrations, peaks around 1482-1163 cm^{-1} attributed to δ_{C-H} of CH_2 and CH_3 groups, peaks around 1075 and 1010 cm^{-1} attributed to ν_{C-O} and peaks around 972-737 cm^{-1} attributed to γ_{C-H} of organic species. [21] In addition to the above characteristic peaks of organic species, there is also a pronounced peak at 846 cm^{-1}, which should be attributed to ν_{P-F} bands, [22] in the FT-IR spectrum of the electrolytes. The FT-IR analysis indicated that the main components of extracts are organic carbonate. The FT-IR spectrum of the extracts is not entirely consistent with the electrolytes', which means a change in the structure of some components. Therefore, further research is needed to identify the each composition of the extracts.

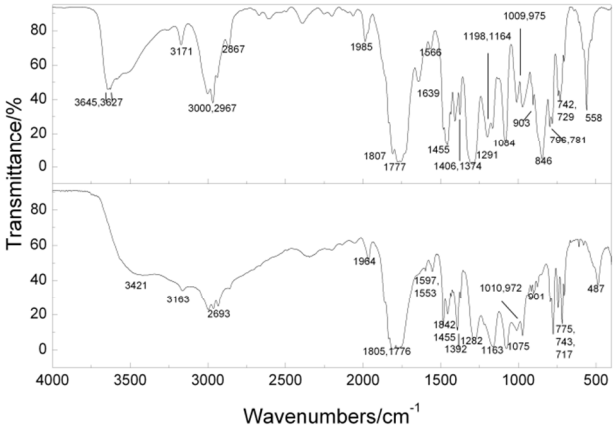

Fig. 3 Comparison between the FT-IR spectrum of electrolyte (top) and extract (bottom)

The volatile components produced in the extraction process of this electrolyte was analyzed by GC-MS and structurally assigned through matching to the National Institutes of Standards (NIST) library. The gas chromatograms of electrolyte components before and after SFE were compared and analyzed to confirm consistency and integrity of electrolyte components. The Figure 4 reveals that electrolytes and extracts have a high degree of consistency in gas chromatographic retention times. There is no significant difference between electrolyte and extracts in components. The extracts in order of volatility (early to late retention times) are characterized as dimethyl carbonate, ethyl methyl carbonate, vinylene carbonate, ethylene carbonate, 1, 11-Biphenyl, which are listed in Table 3.

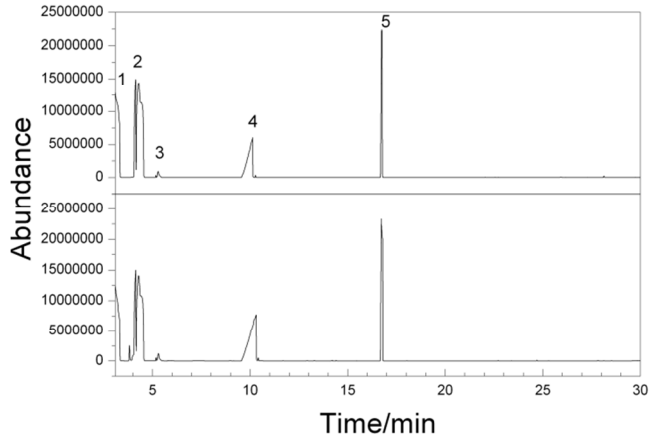

Fig. 4 Comparison between the gas chromatogram of electrolyte (top) and extract (bottom)

Table 3 Components analysis of electrolyte extracts by mass spectrometry in order of volatility was marked in figure 4

No.	Components	Retention times/min	Molecular weight	Molecular ion peak
1	Dimethyl carbonate	3.087	90	90
2	Ethyl methyl carbonate	4.123	103	103
3	Vinylene carbonate	5.282	86	86
4	Ethylene carbonate	10.125	88	88
5	1, 11-Biphenyl	16.736	154	154

Conductive salt

In order to determine the content of $LiPF_6$ in the extracts, the remaining Li^+ concentrations were analyzed using ICP-OES. The results show that the Li^+ concentration in electrolyte solution is 0.9038 mol/L, but only 0.0636 mol/L in extract. Comparing the test results of the two Li^+ concentrations, it turns out that $LiPF_6$ was decomposed during the supercritical CO_2 extraction process.

To further prove that the $LiPF_6$ was hydrolyzed, the electrolyte, soak solution of separator with DMC after SFE and extract were analyzed by nuclear magnetic resonance spectroscopy. The ^{19}F and ^{31}P NMR spectra and peak assignments for above samples are depicted in Figure 5 and 6, respectively. In the ^{19}F NMR spectrum of electrolytes (Fig. 5a), the doublet with chemical shift −72.8 ppm are assigned to PF_6^-, another doublet can be observed at −84.3 ppm are ascribed to $PO_2F_2^-$, which is the product of $LiPF_6$ hydrolysis. In the case of soak solutions of separator with DMC after SFE (Fig. 5b), two doublets at −75.7 ppm and −85.1 ppm are attributed to PO_3F^{2-} and $PO_2F_2^-$, respectively. A singlet of F^- with chemical shift −188.2 ppm was also observed. Furthermore, in the spectrum of extract (Fig. 5c), the same singlet can be found at −187.8 ppm. In the ^{31}P NMR spectrum of electrolytes (Fig. 6a), the septet at −144.3 ppm is ascribed to the PF_6^-. And for the soak solutions of separator with DMC after SFE (Fig. 6b), a singlet and a doublet are observed at 1.3 and −7.4 ppm, which can be assigned to the H_3PO_4 and PO_3F^{2-}, respectively. However, the intensities of the signals are too low to be clearly seen in the spectrum of extract (Fig. 6c). Therefore, only $PO_2F_2^-$, PO_3F^{2-} and HF are detected clearly, other products of hydrolysis cannot be obviously observed. These spectra are similar to the NMR measurements of hydrolysis in propylene carbonate-dimethyl carbonate-H_2O reported by other authors. [23]

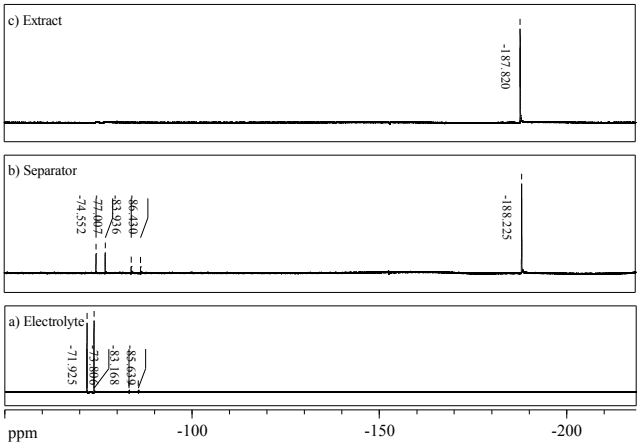

Fig. 5 ^{19}F NMR spectrum of electrolyte, separator and extract in [D_6]Actone (376.4MHz, 25℃)

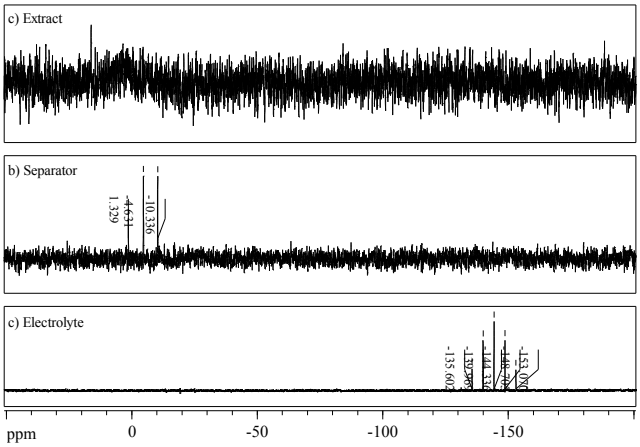

Fig. 6 ^{31}P NMR spectrum of electrolyte, separator and extract in [D_6]Actone (376.4MHz, 25℃)

Generally, $LiPF_6$ is electrolytic dissociative in organic solvents in the equation:

$$LiPF_6 \rightleftharpoons Li^+ + PF_6^- \quad (3)$$

However, Part of non-electrolytic dissociative $LiPF_6$ is instable, and decomposed into LiF and PF_5: [24]

$$LiPF_6 \rightleftharpoons LiF + PF_5 \quad (4)$$

PF_5 is a strong Lewis acid, [25] and hydrolyzed by trace water in the impurity CO_2 according to following equation: [26,27]

$$PF_5 + H_2O \rightleftharpoons POF_3 + 2HF\uparrow \quad (5)$$

$$POF_3 + 3H_2O \rightleftharpoons H_3PO_4 + 3HF\uparrow \quad (6)$$

As intermediates, $PO_2F_2^-$ and PO_3F^{2-} are synthesized in the transformation course of POF_3:[23]

$$POF_3 + H_2O \rightleftharpoons PO_2F_2^- + HF + H^+ \quad (7)$$

$$PO_2F_2^- + H_2O \rightleftharpoons PO_3F^{2-} + HF + H^+ \quad (8)$$

The above analysis and results of the NMR spectra suggest that $LiPF_6$ was hydrolyzed in the extraction process. Some products of

the hydrolysis of $LiPF_6$ were absorbed on the separator, especially the most of phosphorus-containing products of the hydrolysis stayed in the separator. HF, another product of the hydrolysis of $LiPF_6$, will cause damage to both human health and equipment. Therefore, exhaust gas should be treated with appropriate method before emitting into the atmosphere or entering into the CO_2 circulation system. In this study, the HF was absorbed by filtering tube filled with alumina.

Conclusions

The supercritical CO_2 extraction is an efficient and environment-friendly electrolyte separation method for recycling LIBs. The extraction yield of electrolytes from the LIBs separator can achieve $85.07 \pm 0.36\%$ on the mildest operating conditions of 23MPa, 40℃and 45min. This result matched with the predict values confirmed that the response model is adequate to reflect the expected optimization. The experiment results showed that the extraction pressure is the major contributing factor of electrolyte extraction. Besides, the results of component analysis reveal that the contents of organic solvents in electrolyte are basically remained unchanged in the supercritical CO_2 extraction process. The electrolyte is a mixture, and the best choice for the purification and reuse of electrolyte is that the mixture can be selectively extracted into individual component by using the supercritical CO_2. This is the next goal of electrolyte recycling in further research.

Acknowledgement

This research was supported by the National Natural Science Foundation of China (no. 51274075), the National Environmental Technology Special Project (no. 201009028), and Guangdong Province-department University-industry Collaboration Project (grant nos. 2012B091100315). Yuanlong Liu thanks Dr. Zhaohui Wen, at Department of Neuro Intern, First Affiliated Hospital of Harbin Medical University, Harbin, China, for her constant help and suggestions.

Notes and references

School of Chemical Engineering and Technology, Harbin Institute of Technology, Harbin 150001, P.R. China;
*Corresponding authors: Changsong Dai,(Dai C. S., PhD)
E-mail: changsd@hit.edu.cn(Dai C.S.)

1 M. J. Lain, *J Power Sources*, 2001, **97-98**, 736-738.
2 X. Zeng, J. Li and N. Singh, *Crit Rev Env Sci Tec*, 2013, **44**, 1129-1165.
3 M. Vanitha and N. Balasubramanian, *Environmental Technology Reviews*, 2013, **2**, 101-115.
4 O. E. Bankole, C. Gong and L. Lei, *Journal of Environment & Ecology*, 2013, **4**.
5 S. Al-Thyabat, T. Nakamura, E. Shibata and A. Iizuka, *Miner Eng*, 2013, **45**, 4-17.
6 D. Aurbach, A. Zaban, Y. Gofer, Y. E. Ely, I. Weissman, O. Chusid and O. Abramson, *J Power Sources*, 1995, **54**, 76-84.
7 G. E. Blomgren, *J Power Sources*, 1999, **81-82**, 112-118.
8 G. E. Blomgren, *J Power Sources*, 2003, **119-121**, 326-329.
9 K. Hayashi, Y. Nemoto, S. Tobishima and J. Yamaki, *Electrochim Acta*, 1999, **44**, 2337-2344.
10 M. J. Lian, *US Patent Pat.*, US6447669 B1, 2002.
11 M. Schmidt, R. P. Hemmer, M. Wohlfahrt-Mehrens, G. Arnold, Christian Vogler, *US Patent Pat.*, US6511639 B1, 2003.
12 L. Sun and K. Qiu, *J Hazard Mater*, 2011, **194**, 378-384.
13 E. Reverchon and I. De Marco, *The Journal of Supercritical Fluids*, 2006, **38**, 146-166.
14 S. Wang, Y. Ling and Y. Giang, *Forensic Science Journal*, 2003, **2**, 5-18.
15 H. Fu and M. A. Matthews, *J Hazard Mater*, 1999, **67**, 197-213.
16 V. Jain, *Environ Sci Technol*, 1993, **27**, 806-808.
17 S. E. Sloop, *US Patent Pat.*, US7858216 B2, 2010.
18 E. Zinigrad, L. Larush-Asraf, J. S. Gnanaraj, M. Sprecher and D. Aurbach, *Thermochim Acta*, 2005, **438**, 184-191.
19 G. E. P. Box and D. W. Behnken, *Technometrics*, 1960, **2**, 455-475.
20 G. E. P. Box and K. B. Wilson, eds. S. Kotz and N. Johnson, Springer New York, Editon edn., 1992, pp. 270-310.
21 B. Zhang, Y. Zhou, X. Li, X. Ren, H. Nian, Y. Shen and Q. Yun, *Spectrochimica Acta Part A: Molecular and Biomolecular Spectroscopy*, 2014, **122**, 59-64.
22 D. Aurbach, B. Markovsky, A. Shechter, Y. Ein Eli and H. Cohen, *J Electrochem Soc*, 1996, **143**, 3809-3820.
23 A. V. Plakhotnyk, L. Ernst and R. Schmutzler, *J Fluorine Chem*, 2005, **126**, 27-31.
24 L. Terborg, S. Weber, F. Blaske, S. Passerini, M. Winter, U. Karst and S. Nowak, *J Power Sources*, 2013, **242**, 832-837.
25 K. O. Christe, D. A. Dixon, D. McLemore, W. W. Wilson, J. A. Sheehy and J. A. Boatz, *J Fluorine Chem*, 2000, **101**, 151-153.
26. D. Aurbach, A. Zaban, Y. Ein-Eli, I. Weissman, O. Chusid, B. Markovsky, M. Levi, E. Levi, A. Schechter and E. Granot, *J Power Sources*, 1997, **68**, 91-98.
27 T. Kawamura, S. Okada and J. Yamaki, *J Power Sources*, 2006, **156**, 547-554.

Figure captions

Fig. 1 Schematic diagram of supercritical CO_2 extraction apparatus: 1 CO_2 Cylinder, 2 Cooling Bath, 3 Air Driven Fluid Pump (gas booster pump), 4Air Compressor, 5 Air Regulator, 6 CO_2 Pressure, 7 Inlet Valve, 8 Extraction Vessel, 9 Heating Jacket, 10 Vessel Heat, 11 Vent Valve, 12 Outlet Valve, 13 Flow Valve, 14 Valve Heat, 15 Heating Jacket, 16 Collecting Vial, 17 Alumina filter, 18 Gas Flow meter

Fig. 2 Response surfaces and contour plots for: (a) Extraction time vs. Pressure; (b) Extraction time vs. Temperature.

Fig. 3 Comparison between the FT-IR spectrum of electrolyte (top) and extract (bottom)

Fig. 4 Comparison between the gas chromatogram of electrolyte (top) and extract (bottom)

Fig. 5 ^{19}F NMR spectrum of electrolyte, separator and extract in [D_6]Actone (376.4MHz, 25℃)

Fig. 6 ^{31}P NMR spectrum of electrolyte, separator and extract in [D_6]Actone (376.4MHz, 25℃)

Figures

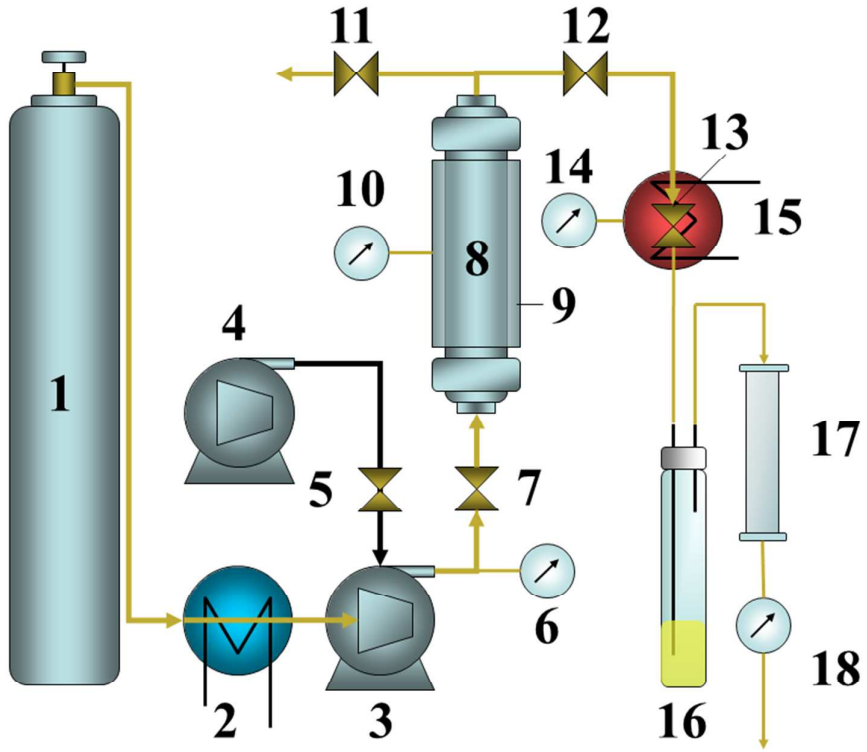

Fig. 1 Schematic diagram of supercritical CO_2 extraction apparatus: 1 CO_2 Cylinder, 2 Cooling Bath, 3 Air Driven Fluid Pump (gas booster pump), 4Air Compressor, 5 Air Regulator, 6 CO_2 Pressure, 7 Inlet Valve, 8 Extraction Vessel, 9 Heating Jacket, 10 Vessel Heat, 11 Vent Valve, 12 Outlet Valve, 13 Flow Valve, 14 Valve Heat, 15 Heating Jacket, 16 Collecting Vial, 17 Alumina filter, 18 Gas Flow meter

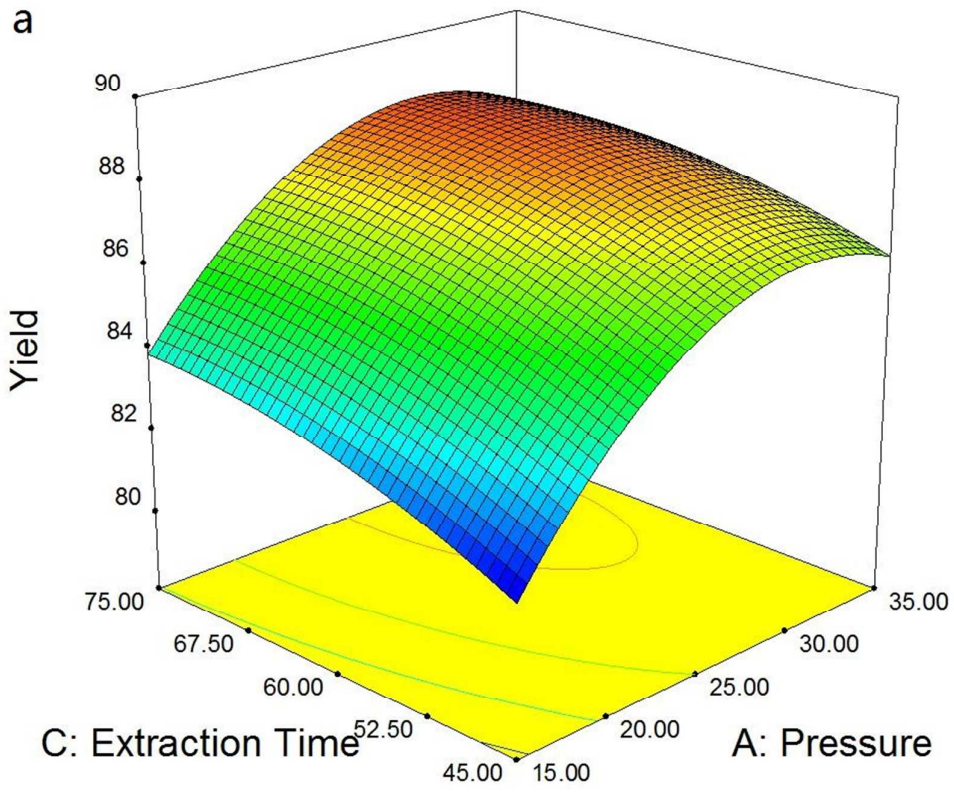

1

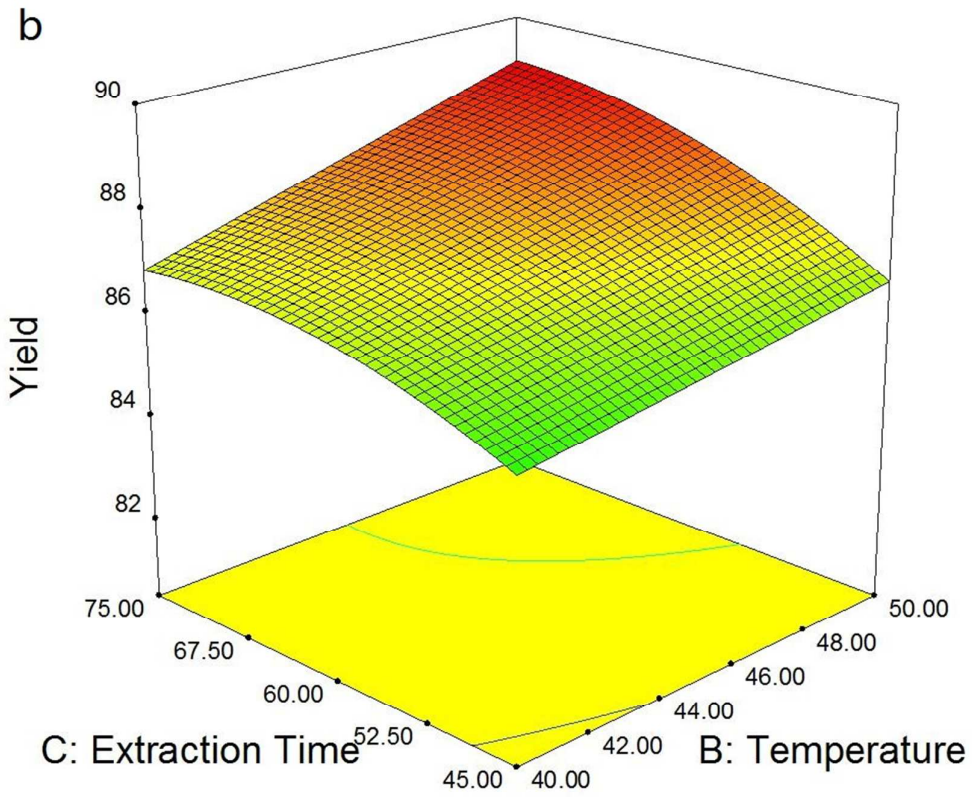

Fig. 2 Response surfaces and contour plots for: (a) Extraction time vs. Pressure; (b) Extraction time vs. Temperature.

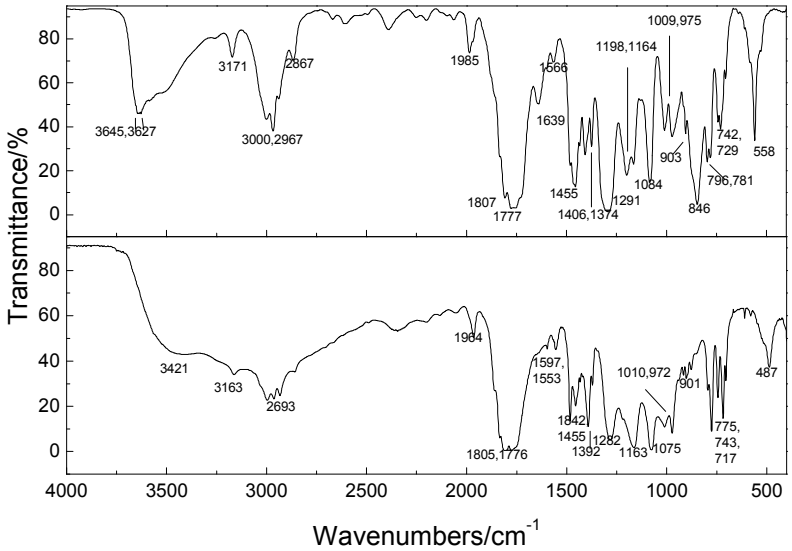

Fig. 3 Comparison between the FT-IR spectrum of electrolyte (top) and extract (bottom)

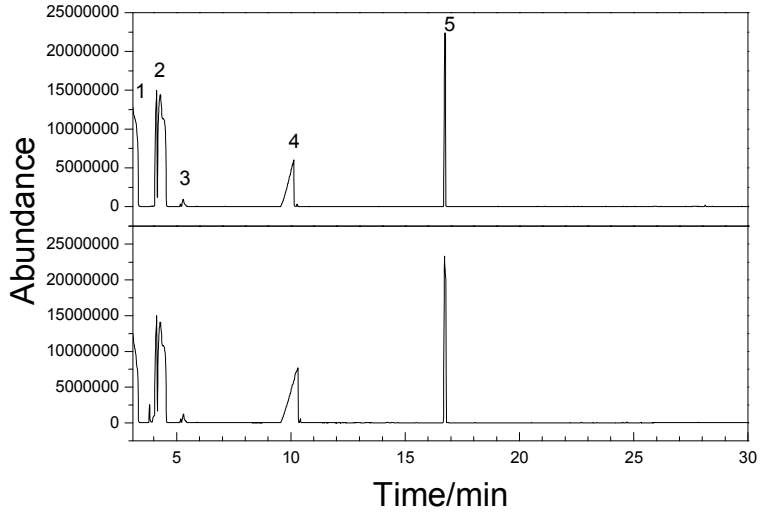

Fig. 4 Comparison between the gas chromatogram of electrolyte (top) and extract (bottom)

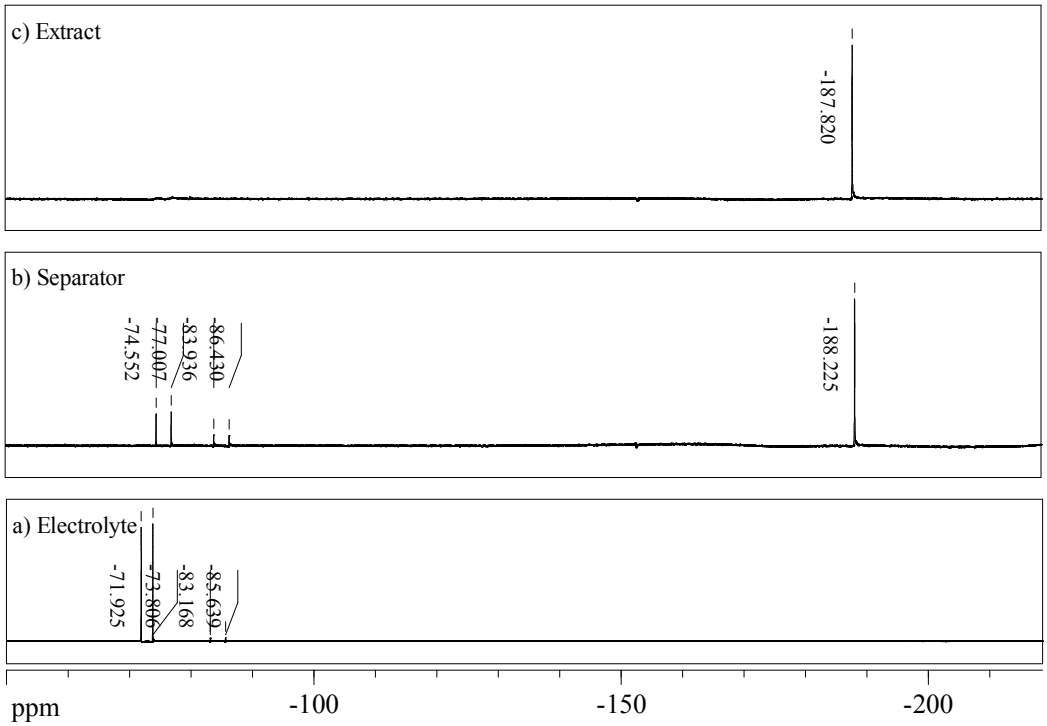

Fig. 5 ^{19}F NMR spectrum of electrolyte, separator and extract in [D_6]Actone (376.4MHz, 25℃)

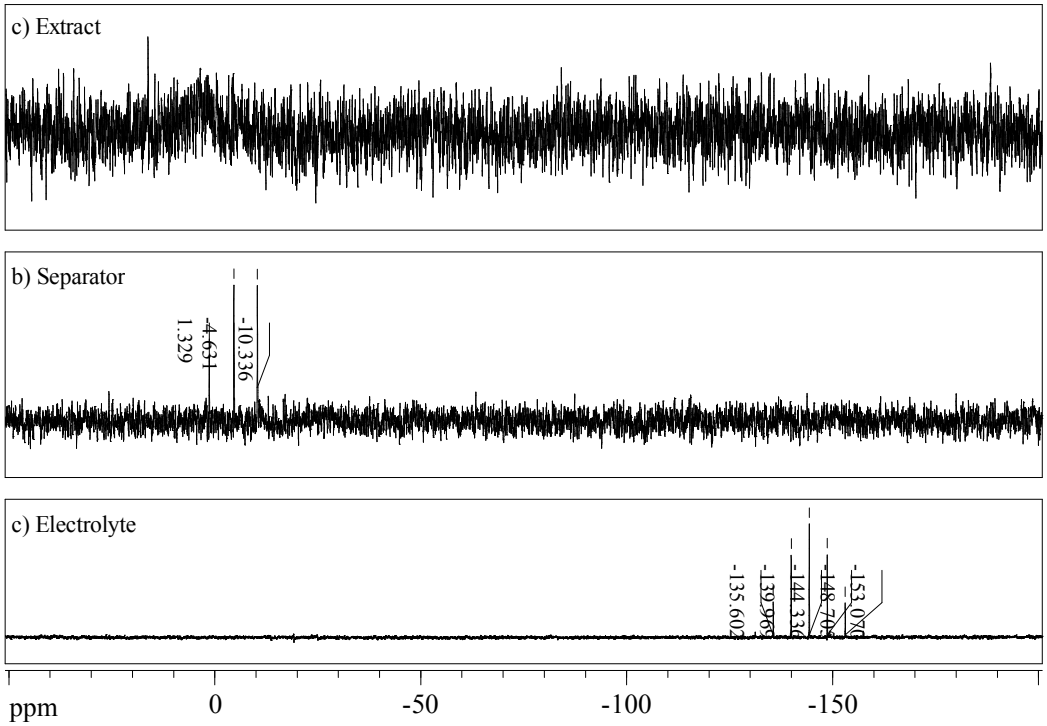

Fig. 6 ^{31}P NMR spectrum of electrolyte, separator and extract in [D_6]Actone (376.4MHz, 25℃)